Nucleate Pool Boiling CFD simulation

Yanis Mondet

November 18, 2024

Abstract

This report present the development a CFD simulation for modelling nucleate pool boiling on OpenFOAM. It take place in the course Numerical project at Grenoble INP - ENSE3.

1 Introduction

Boiling phenomena occur in a wide range of engineering applications, such as vapor generators in a nuclear power plants. Understanding boiling is crucial for optimizing these systems. However, boiling heat transfert is highly complex and no full comprehensive theory currently describes boiling across all conditions and applications. Boiling heat transfert can be studied at different lenght scales, from individual bubble dynamics to interaction between water and vapor phases.

One approach for simulating boiling is Computational FLuid Dynamics (CFD) simulation. In this project, boiling is studied through numercial simulatiosn at the scale of a single bubble. The open-source software OpenFOAM version V2106 was used, employing and modifying a solver developped by Municchi and Magnini [1].

This report first presents an overview of boiling modelling and a description of the numerical model used for this simulation. Then, the bubble detachment studied by Georgoulas et al. [2] is reproduced and the influence of various parameters is studied and their effects is compared on the boiling process.

2 Boiling modelling

2.1 Basic knowledge about multiphase flow modelling

Since in our case we don't need to folow the bubble we are going to use an Eulerain model. There are two possible model: VOF method or the Euler-Euler model. Firstly, we are going to use the VOF method in order to simulate the flow.

The **Volume of Fluid (VOF)** model is used to track and locate the interface between two immiscible fluids, such as liquid and vapor, in multiphase flow simulations. The VOF model introduces a **volume fraction field** α to represent the presence of each fluid in a computational cell.

The volume fraction α represents the fraction of the cell occupied by the liquid phase:

$$\alpha = \begin{cases} 1, & \text{cell fully liquid} \\ 0, & \text{cell fully vapor} \\ 0 < \alpha < 1, & \text{interface region (mixed cell)} \end{cases}$$

The interface is represented by cells where $0 < \alpha < 1$. In these mixed cells, the interface can be approximated using techniques like the Piecewise Linear Interface Calculation (PLIC), which provides an accurate representation of the boundary between the phases.

In cells containing the interface, the fluid properties such as density ρ and viscosity μ are computed as weighted averages based on α:

$$\rho = \alpha\rho_l + (1-\alpha)\rho_v, \tag{1}$$

$$\mu = \alpha\mu_l + (1-\alpha)\mu_v, \tag{2}$$

where ρ_l and μ_l are the properties of the liquid phase, and ρ_v and μ_v are the properties of the vapor phase.

2.2 Governing Equation for VOF

2.2.1 Volume fraction equation

The volume fraction equation is:

$$\frac{\partial \alpha}{\partial t} + \nabla \cdot (\alpha \mathbf{u}) = -\frac{1}{\rho_1} m_i'' \nabla \alpha$$

where:
- α: volume fraction of liquid phase (ranges from 0 for vapor to 1 for liquid),
- $\mathbf{u}$: velocity vector of the flow,
- m_i'': phase change rate per unit area (interface mass flux, measured in kg/m^2/s),
- ρ_1: density of the liquid phase.

This equation describes how the volume fraction of the liquid phase changes due to advection and phase change at the interface.

2.2.2 Incompressibility Condition

The incompressibility condition is modified to account for phase change, incorporating densities of both phases:

$$\nabla \cdot \mathbf{u} = \frac{1}{\rho_2} - \frac{1}{\rho_1} m_i'' \nabla \alpha$$

where ρ_2 is the density of the vapor phase.
This ensures that the divergence of velocity considers the density difference due to phase transition between liquid and vapor.

2.2.3 Energy Equation

The energy conservation equation integrates conductive and convective heat transfer with latent heat effects at the phase boundary:

$$\frac{\partial (\rho c_p T)}{\partial t} + \nabla \cdot (\rho c_p \mathbf{u} T) = \nabla \cdot (\lambda \nabla T) - m_i'' h_{lv} \nabla \alpha$$

where:
- T: temperature,
- c_p: specific heat capacity,
- λ: thermal conductivity,
- h_{lv}: latent heat of vaporization.

This equation models the thermal behavior of the system, incorporating both the heat diffusion in the bulk phases and the heat required for phase change at the interface.

2.2.4 Momentum Conservation (Navier-Stokes Equation)

The momentum equation includes terms for pressure, viscosity, and surface tension at the interface:

$$\frac{\partial (\rho \mathbf{u})}{\partial t} + \nabla \cdot (\rho \mathbf{u} \mathbf{u}) = -\nabla p + \nabla \cdot \tau + \mathbf{F}_\sigma$$

where:
- p: pressure,
- τ: viscous stress tensor,
- $\mathbf{F}_\sigma$: surface tension force.

2.2.5 Surface tension force

For the surface tension forec we use the Continuum Surface Force (CSF) model given by:

$$\mathbf{F}_\sigma = 2\frac{\rho}{\rho_l + \rho_v}\sigma\kappa\nabla\alpha$$

where: - σ: surface tension coefficient, - κ: interface curvature, - ρ: effective density based on the volume fraction, $\rho = \rho_2 + (\rho_1 - \rho_2)\alpha$.

2.2.6 Interface Conditions

The **interface indicator function** I specifies the phase (liquid or vapor) at each point, defined as:

$$I(\mathbf{x}, t) = \begin{cases} 1, & \text{in liquid} \\ 0, & \text{in vapor} \end{cases}$$

The volume fraction α is then calculated by integrating I over a control volume V:

$$\alpha = \frac{1}{V}\int_V I(\mathbf{x}, t)dV$$

This function determines the local phase within the control volume and guides phase change computations by indicating where α transitions.

2.2.7 Phase Change with the Hardt and Wondra Model

The interfacial mass flux m_i'' is modeled according to Hardt and Wondra:

$$m_i'' = \frac{h_i}{h_{lv}}(T_i - T_{sat}) \tag{3}$$

where:

- T_i is the temperature at the interface.
- T_{sat} is the saturation temperature at the interfacial pressure.
- h_i is the interfacial heat transfer coefficient given by:

$$h_i = \left(\frac{2\gamma}{2-\gamma}\right)\rho_v h_{lv}\left(\frac{\bar{M}}{2\pi\bar{R}}\right)^{1/2}\left(\frac{p_v}{T_{sat}^3}\right)^{1/2} \tag{4}$$

- γ is an accommodation coefficient (typically between 0 and 1).
- $\bar{M}$ is the molar mass.
- $\bar{R}$ is the universal gas constant.
- p_v is the vapor pressure at the interface.

Together, these equations govern the conservation of phase fraction, momentum, and energy in the "boilingFoam" solver, allowing it to accurately simulate phase change dynamics such as boiling and condensation by resolving heat transfer, interface movement, and density differences across phases.

3 Numerical model validation

To validate the solver, a test case included in the solver was tested and subsequently adapted to different configurations, with the results compared to analytical solutions.

3.1 Bubble Growth Theory

Bubble growth is a basic test case used to validate multiphase solver, Scriven [3] developped a numerical solution for bubble growth in a saturated liquid. The bubble radius $R(t)$ follows the law:

$$R(t) = 2\beta\sqrt{D\,t}, \tag{5}$$

where β is given by:

$$\beta = J_a\sqrt{\frac{3}{\pi}}, \tag{6}$$

and the Jacob number J_a is defined as:

$$J_a = \frac{(T_\infty - T_{\text{sat})}\rho_l c_{p,l}}{\rho_v h_{l,v}}. \tag{7}$$

This boundary layer, derived from thermal diffusion theory (without additional heat sources), is defined by the following equation:

$$\delta = 2\sqrt{Dt}, \tag{8}$$

where D is the thermal diffusivity and t is the time required for the bubble to reach its current size. Using this formula in combination with the Scriven radius equation, we obtain:

$$\delta = \frac{R(t)}{\beta}, \tag{9}$$

where R is the bubble radius and β is a growth factor.

3.2 Test Cases

3.2.1 Definition of General Parameters

After testing the solver with the included test cases, we modified one of them to simulate bubble growth in saturated water with a temperature difference (ΔT) of 5°C. A 2D axisymmetric geometric approach is employed due to limited computational power. A bubble with an initial diameter of 100 μm is expected to grow to 500 μm within 2 ms. The initial conditions consist of a vapor bubble at 373.15 K surrounded by liquid at 378.15 K. To ensure both convergence and physical accuracy, the initial thermal boundary layer δ is added as an initial condition.

The boundary conditions (BC) for this simulation are as follows:

- **Axis (Left Boundary):** Symmetry boundary condition, implying no flux across this boundary. This reduces the computation to half of the domain.
- **Top Boundary:**
  - Fixed value for pressure (P)
  - Zero gradient for α (volume fraction), T (temperature), and U (velocity)
- **Right Boundary:**
  - Fixed value for pressure (P)
  - Zero gradient for α, T, and U
- **Bottom Boundary:** Symmetry boundary condition

To validate the solver while keeping computation times manageable, we limit the simulation to the first 0.4 ms of growth. This allows for a smaller domain and reduces the overall calculation time. We conduct a mesh convergence analysis using a structured square mesh, as shown in the Figure 1. The domain size is set to $L = 0.5$ mm, ensuring that the bubble remains smaller than half the domain size throughout the simulation.

Property	**Unit**	**Liquid**	**Vapour**
Density, ρ	$\mathrm{kg\,m^{-3}}$	958	0.597
Specific heat capacity, c_p	$\mathrm{J\,kg^{-1}\,K^{-1}}$	4220	2030
Thermal conductivity, k	$\mathrm{W\,m^{-1}\,K^{-1}}$	0.679	0.025
Dynamic viscosity, μ	$\mathrm{Pa\,s}$	2.77×10^{-4}	1.30×10^{-5}
Heat of vaporization, h_{lv}	$\mathrm{J\,kg^{-1}}$	2,257,000	
Surface tension, σ	$\mathrm{N\,m^{-1}}$	0.059	
Saturation temperature, T_{sat}	K	373.15	
Pressure, P	bar	1.013	
Growth constant, β	-	14.59	
Initial thermal layer thickness, δ_{therm}	m	7.00×10^{-6}	
Thermal diffusivity, D	$\mathrm{m^2\,s^{-1}}$	1.68×10^{-7}	
Superheat, ΔT	K	5	
Additional Simulation Parameters			
Initial bubble diameter	µm	100	
Target bubble diameter	µm	500	
Simulation time	ms	0.4	
Domain size, L	mm	0.5	
Temperature inside bubble	K	373.15	
Temperature in liquid	K	378.15	
Courant number (CFL)	-	0.2	
Mesh size, Δ_x	µm	1–2	

Table 1: Summary of Parameters for Bubble Growth Simulation

A crucial parameter in CFD simulations is the Courant–Friedrichs–Lewy (CFL) number. After testing various Courant numbers, we observed that a CFL of 0.02 provides high accuracy but results in very long computation times. Conversely, a CFL of 1 speeds up the calculation but leads to poor resolution, with deformations observed at the bubble boundary, as shown in the Figure 2.

Ultimately, a Courant number of 0.2 was chosen as a good balance between accuracy and computation time.

Finally, I attempted to double the size of the initial boundary layer for a square mesh with cells of 2 μm, see 3. Doubling the initial thermal boundary layer thickness accelerates the computation time since the thermal gradient is smaller when the boundary layer (BL) larger. Initially, the larger BL appears to yield better results. However, the could be due to random variation and futher investiguation is required to confirm this observation. For the remainder of the study, we will keep using the thermal BL determined based on Scriven's theory.

3.2.2 Mesh convergence

Returning to the initial temperature difference (ΔT) of 5°C, we proceed with mesh convergence testing. As seen in the Figure 1, a mesh size Δ_x of 1 μm, mesh 500x500, provides precise results but requires 5 hours to simulate just 0.4 ms of bubble growth. A mesh size of 2 μm, 250x250, though less accurate, reduces the computation time to 45 minutes. A compromise between precision and efficiency has to be found according to what we want to study. Mesh cells of 1μm result in an error below 5%, whareas mesh cells of 2μm produce an error of approximately 30%.

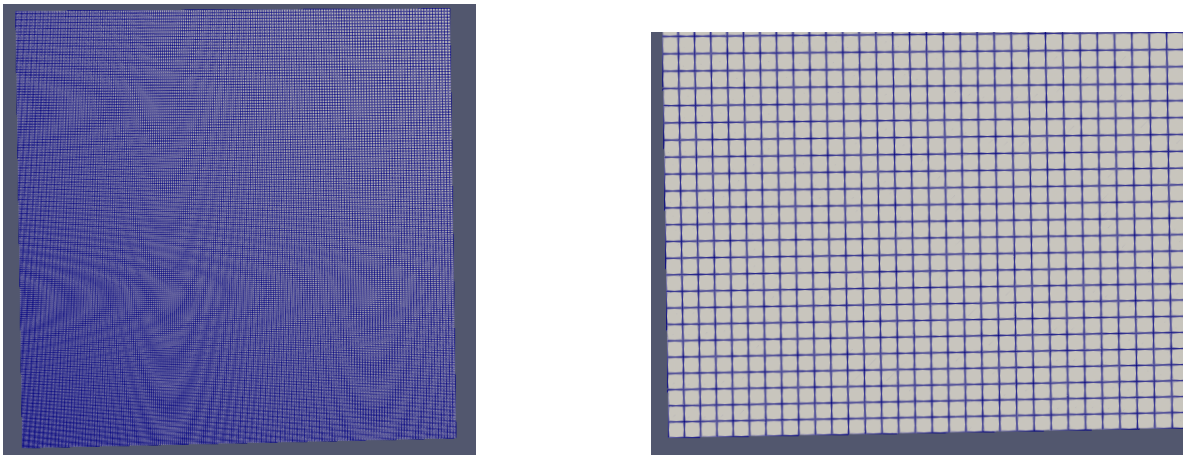

(a) Global Mesh (b) Local Mesh

Figure 1: Comparison of Global and Local Meshes

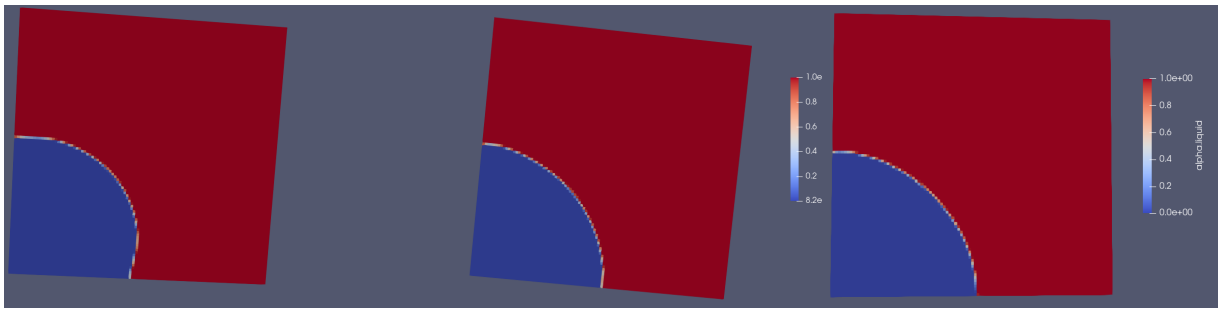

(a) CFL = 1 (b) CFL = 0.2 (c) CFL = 0.02

Figure 2: Comparison of CFL conditions at different settings.

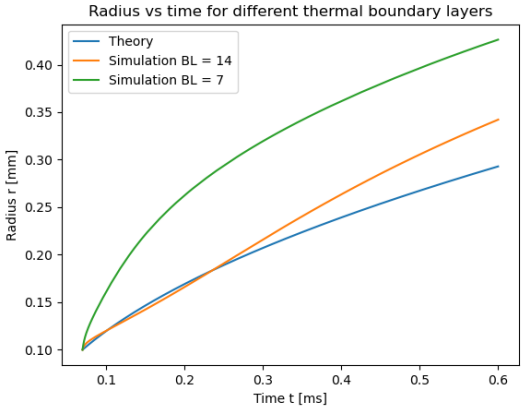

Figure 3: Initial BL impact on the results

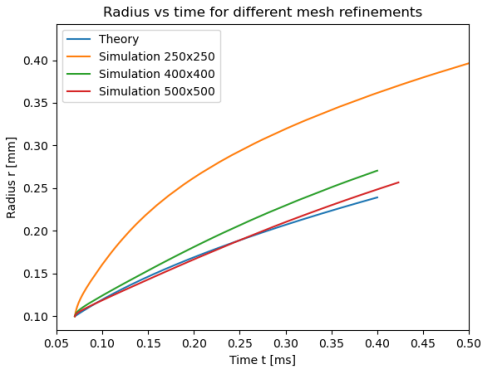

(a) Growth convergence

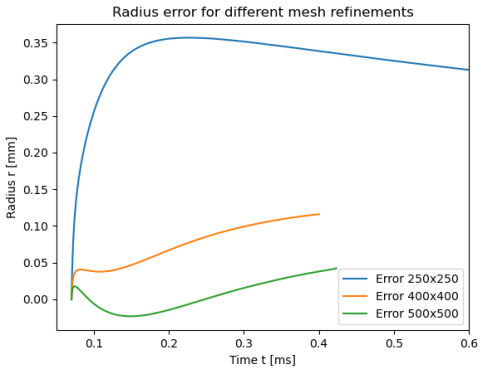

(b) Error du to the convergence

Figure 4: Comparison of mesh convergence for radius and errors.

3.3 Study of bubble detachment

Knowing that our solver gives good results and having done various hypothesis on the parameters in order to save computation time. This part concentrate on the bubble detachment in a pool boiling configuration for saturated R113. The parameters of this study are listed in the Table 2.

Phase Properties (R113 at 1 bar, $T_{\text{sat}} = 320.65\,\text{K}$)			
Property	**Unit**	**Liquid**	**Vapour**
Density, ρ	$\text{kg}\,\text{m}^{-3}$	1508.4	7.4
Specific heat, c_p	$\text{J}\,\text{kg}^{-1}\,\text{K}^{-1}$	940.3	691.3
Thermal conductivity, k	$\text{W}\,\text{m}^{-1}\,\text{K}^{-1}$	0.064	0.0095
Kinematic viscosity, ν	$\text{m}^2\,\text{s}^{-1}$	3.25×10^{-7}	1.39×10^{-6}
Surface tension, σ	$\text{N}\,\text{m}^{-1}$	0.015	
Latent heat, h_{lv}	$\text{J}\,\text{kg}^{-1}$	144,350	
Initial Conditions			
Initial bubble radius	µm	50	
Initial thermal boundary layer thickness	µm	352	
Temperature difference, ΔT	K	13.5	
Contact angle	°	30	
Domain size	mm	2.5×4.0	
Simulation type	-	Axisymmetric	
Number of computational cells	-	400,000	

Table 2: Summary of Simulation Parameters

References

[1] Fmuni. GitHub - fmuni/boilingFoam-PUBLIC: OpenFOAM-based solvers, libraries, and test cases for simulating boiling flows.

[2] Anastasios Georgoulas, Manolia Andredaki, and Marco Marengo. An Enhanced VOF Method Coupled with Heat Transfer and Phase Change to Characterise Bubble Detachment in Saturated Pool Boiling. *Energies*, 10(3):272, 2 2017.

[3] L.E. Scriven. On the dynamics of phase growth. *Chemical Engineering Science*, 10(1):1–13, 1959.